

A new dynamical mechanism of incomplete fusion in heavy-ion collision

A.K. Nasirov^{1,2,*}, B.M. Kayumov^{2,3}, O.K. Ganiev^{2,4,5}, and G.A. Yuldasheva²

¹*Joint Institute for Nuclear Research, 141980 Dubna, Russia*

²*Institute of Nuclear Physics, Uzbekistan Academy of Sciences, 100214 Tashkent, Uzbekistan*

³*New Uzbekistan University, 100007 Tashkent, Uzbekistan*

⁴*School of Engineering, Akfa University, 111221 Tashkent, Uzbekistan*

⁵*Faculty of Physics, National University of Uzbekistan, 100174 Tashkent, Uzbekistan*

(Dated: February 8, 2023)

The incomplete fusion has been proved as the formation and emission of the α particle by the increase in the rotational energy of the very mass-asymmetric dinuclear system. The results of the dinuclear system model have confirmed that the incomplete fusion in heavy-ion collisions occurs at a large orbital angular momentum ($L > 30\hbar$) due to the strong increase of the intrinsic fusion barrier.

The incomplete fusion (ICF) of nuclei at the heavy-ion collision is observed in reactions of light projectiles with the intermediate-mass target nucleus. This phenomenon was first observed more than 60 years ago [1]. From the analysis of experimental data it was found that the peripheral collisions are a favorable condition for the incomplete fusion. This phenomenon is studied by observation of the α particle flying in the forward angles or other light clusters or by identification of the evaporation residue accompanied with the emitted fast light clusters.

A mean value $\langle L \rangle = 40\hbar$ of the angular momentum distribution of the entrance channel corresponding to the incomplete fusion was observed for the $^{159}\text{Tb}(^{14}\text{N}, \alpha xn)^{169-x}\text{Yb}$ reaction [2], while the estimated value $\langle L \rangle = 30\hbar$ was presented in Ref. [3] for the $^{16}\text{O}+^{146}\text{Nd}$ reaction. The cross section of the evaporation residues (ER) formed in the incomplete fusion increases gradually with the mass asymmetry of the reaction entrance channel [4]. The ER presence accompanied with the emission of the α particle formed in the incomplete fusion has been established from the analysis of the total cross section for the α -particle production by the standard statistical models ALICE-91 [4] and PACE4 [5, 6]. The conclusion of the authors is based on the enhancing underestimation of the measured cross sections of α -emitting residues by the theoretically predicted cross sections.

The breakup fusion model [7] was suggested to describe ICF. In this model, the projectile is assumed to break up into a light cluster and a conjugate nucleus at close distances to the target nucleus.

The sum-rule model [8, 9] developed by Wilczynski *et al.* was used to calculate the ER cross section of various projectile-like fragments formed in ICF reactions. The authors concluded that ICF reactions are localized in the angular momentum space above the critical angular momentum ℓ_{cr} for complete fusion (CF) of projectile and target.

The breakup of the projectile was analysed in the recent paper [10] by R. V. den Bosshe and A.D. Torres by combining a classical trajectory model with stochastic breakup with the quantum-mechanical fragmentation

theory [11] treatment of two-body clusterization and decay of a projectile. The angular distributions of the clusters ^4He and ^8Be produced at the breakup of projectile in the $^{20}\text{Ne}+^{208}\text{Pb}$ reactions explored and compared with the experimental data.

We should stress that the projectile breakup mechanism of the incomplete fusion was assumed in all of the above-listed theoretical methods to analyse measured data.

In this work, we consider a new mechanism of the ICF reaction as a quasifission to calculate the excitation function of the evaporation residues (ER) survived against fission, which is accompanied by the α -particle emission from the dinuclear system (DNS) (see Fig. 1). The DNS is formed at the capture (full momentum transfer) of the projectile nucleus by the target nucleus.

This mechanism is based on the DNS concept of the complete fusion which operates with such physical quantities as intrinsic fusion barrier B_{fus}^* , quasifission barrier B_{qf} and the excitation energy E_Z^* of the DNS with the charge asymmetry Z . The DNS evolution by the diffusion process due to the nucleon transfer between fragments leads to the formation of the α particle in collisions with the large orbital angular momentum if capture takes place at the given beam energy.

The increase of the orbital angular momentum in the entrance channel leads to the following changes of the physical quantities causing the enhance of the incomplete fusion probability.

i) The increase of the dynamical intrinsic barrier B_{fus}^* to complete fusion at the very asymmetric charge and mass distribution corresponding to the α particle (see Figs. 2 and 3).

ii) The decrease of the stability of the DNS due to decrease the depth of the potential well of the nucleus-nucleus interaction. It is called the quasifission barrier B_{qf} (see Fig. 2).

iii) The excitation energy E_Z^* of the DNS with the charge asymmetry Z , which is generated from the total kinetic energy loss at the capture of the projectile by the target nucleus, decreases due to increase the DNS rotational energy (see Fig. 2). Therefore, the residue nucleus formed in the incomplete fusion is less heated than the compound nucleus formed in the complete fusion.

* nasirov@jinr.ru

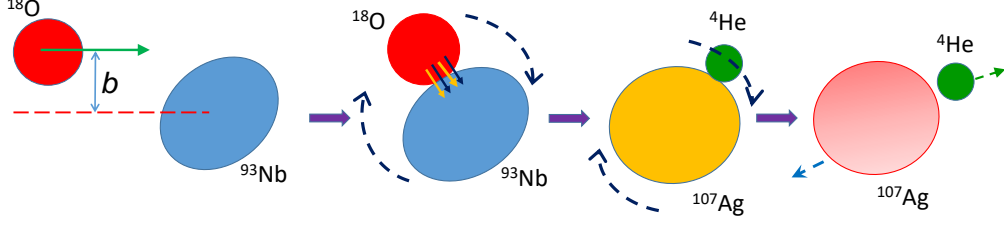


FIG. 1. The sketch of the incomplete fusion mechanism as very asymmetric quasifission in the case of the $^{18}\text{O}+^{93}\text{Nb}$ reaction.

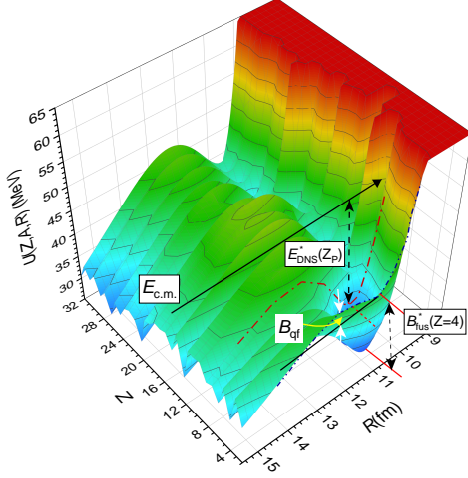


FIG. 2. Potential energy surface calculated for the DNS formed in the $^{16}\text{O}+^{130}\text{Te}$ reaction at the collisions with the values of orbital angular momentum $L = 40\hbar$ as a function of the fragment charge numbers (Z) and relative distance (R) between centres-of-mass fragments. The DNS excitation energy $E_{\text{DNS}}^*(Z_P)$, the intrinsic fusion B_{fus}^* barrier is shown for $Z = 4$ and quasifission B_{qf} barrier is shown for $Z = 2$ by the corresponding arrows.

iv) The effect of the centrifugal force on the very mass-asymmetric DNS enhances leading to the incomplete fusion which can be considered as the DNS quasifission producing very mass-asymmetric products.

The potential energy surface (PES) presented in Fig. 2 is calculated as a sum of the nucleus–nucleus interaction V and reaction energy balance Q_{gg} [12]:

$$U(Z, A, L, R, \{\beta_i, \alpha_i\}) = Q_{gg} - V_{\text{rot}}^{\text{CN}}(L) + V(Z, A, L, R, \{\alpha_i, \beta_i\}) \quad (1)$$

where Z and A are charge and mass numbers, respectively, of a DNS fragment, and the ones of the conjugate fragment are $Z_c = Z_{\text{CN}} - Z$ and $A_c = A_{\text{CN}} - A$; $Q_{gg} = B_1 + B_2 - B_{\text{CN}}$ is the reaction energy balance; B_1 , B_2 , and B_{CN} are the binding energies of the interacting nuclei and CN, respectively, which are obtained from the nuclear mass tables in Refs. [13, 14]; β_i and α_i represent deformation parameters (quadrupole and octupole) of the DNS fragments and orientation angles of the axial symmetry axis of the deformed nuclei to the beam direc-

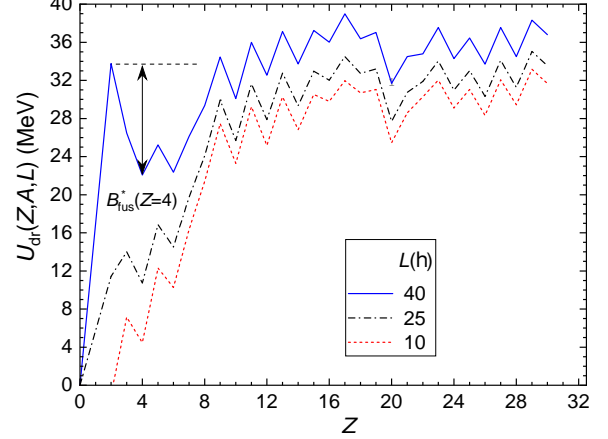


FIG. 3. The driving potential of the DNS formed in the $^{16}\text{O}+^{130}\text{Te}$ reaction calculated for the orbital angular momentum $L = 10, 25, \text{ and } 40\hbar$. the intrinsic fusion B_{fus}^* and quasifission B_{qf} barriers of the entrance channel Z_P are shown by the corresponding arrows.

tion, respectively. In case of the nuclei with at spherical shape at their ground state, the change in their shape due to surface vibration at the zero-point motion is considered [12]. The amplitudes of vibrations are taken equal to the values of the deformation parameters of the first quadrupole 2^+ and octupole 3^- collective excitations of nuclei (β_2^+) [15] and (β_3^-) [16].

The dependence of the barrier B_{fus}^* on L is seen from the analysis Fig. 2 which shows the PES values for the very asymmetric charge asymmetry ($Z \rightarrow 2$ and $Z_c \rightarrow 58$) increase strongly with L due to smallness of the moment of inertia DNS with the α particle. Therefore, the fusion probability decreases by the increase of L , since the intrinsic fusion barrier B_{fus}^* increases and quasifission barrier B_{qf} decreases (see Fig. 2) by increasing L . This circumstance is a reason leading to the creation of the favorable range of the angular momentum for the incomplete fusion in the peripheral collisions at the large beam energies. The enhance of the rotational energy in the PES with L is related with the strongly decrease of moment of inertia of the very asymmetric DNS: $J_{\text{DNS}}(Z, A, Z_c, A_c) = \mu R_m^2 + (J_1(Z, A) + J_2(Z_c, A_c))/2$,

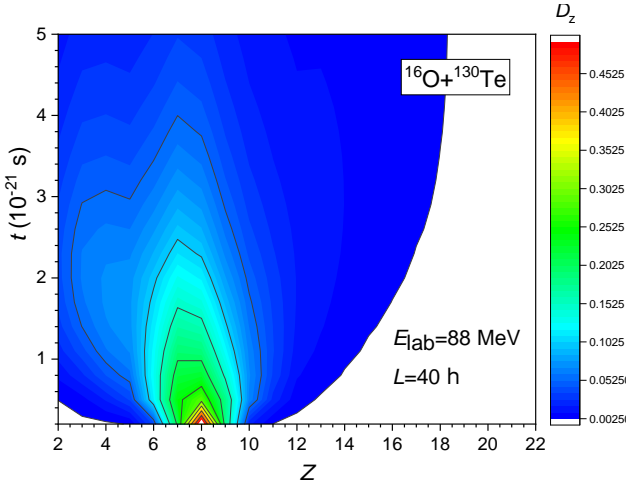


FIG. 4. Evolution of the charge distribution for the projectile-like fragments for the $^{16}\text{O}+^{130}\text{Te}$ reaction at $E_{c.m.} = 78.4$ MeV and $L = 40\hbar$. The results have been obtained for the orientation angles $\alpha_1 = 45^\circ$ and $\alpha_2 = 30^\circ$.

which is used in calculation of the rotational energy:

$$V_{\text{rot}}(Z, A, Z_c, A_c, L, R) = \frac{L(L+1)}{2J_{\text{DNS}}(Z, A, Z_c, A_c)}. \quad (2)$$

The reduced mass of DNS and moments inertia of the interacting nuclei are calculated by the expressions $\mu = mA A_c / (A + A_c)$, $J_1 = 1/5mA(a_1^2 + b_1^2)$ and $J_2 = 1/5mA_c(a_2^2 + b_2^2)$, respectively; m is a nucleon mass; a_i and b_i are small and large radii of nuclei; R_m is the distance corresponding to the minimum of the potential well of the nucleus–nucleus interaction; α_i and β_i are the orientation angle of the axial symmetry axis and the deformation parameter of the DNS fragments, respectively.

The excitation energy E_Z^* of DNS at the given value of the beam energy is calculated taking into account the change in the intrinsic energy of DNS at the change of nucleon numbers of fragments:

$$E_Z^*(E_{c.m.}, A, L, \{\beta_i, \alpha_i\}) = E_{c.m.} + \Delta Q_{\text{gg}}(Z, A) - V(Z, A, R_m, L, \{\beta_i, \alpha_i\}), \quad (3)$$

where $\Delta Q_{\text{gg}}(Z, A) = B + B_c - B_P - B_T$; B_P , B_T , B and B_c are binding energies of the initial (“P” and “T”) and interacting fragments; $V(Z, A, R_m, L, \{\beta_i, \alpha_i\})$ is the minimum value of the potential well, and it is a function of the nuclear shape β_i and orientation angles α_i of the axial symmetry axis of the deformed nuclei to the beam direction [17]. The probability of the α -particle formation and its yield has been estimated as a quasifission fragment by the formula

$$Y_Z(E_Z^*, A, L, t) = \Lambda_Z^{\text{qf}}(B^{\text{qf}}(Z, A, \{\alpha_i, \beta_i\}), T_Z(A, \alpha_i, \beta_i)) \times \sum_{k=0}^{k_{\text{max}}} D_Z(A, E_Z^*, L, t_0 + k\Delta t) \quad (4)$$

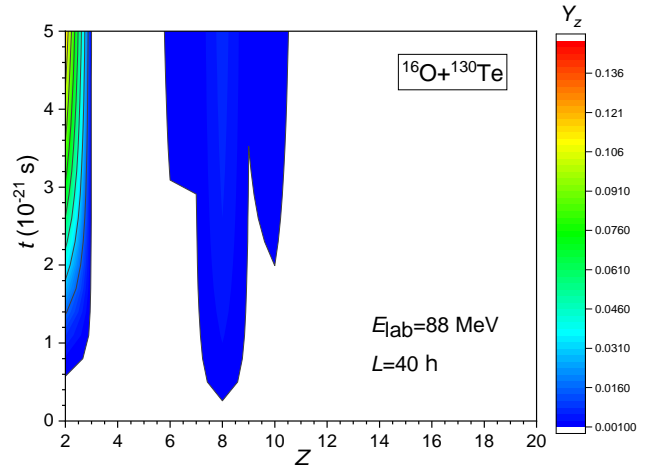


FIG. 5. Evolution of the yield of α particle $Y_Z(Z=2)$ calculated for the $^{16}\text{O}+^{130}\text{Te}$ reaction at $E_{c.m.} = 78.4$ MeV and $L = 40\hbar$. The results have been obtained for the orientation angles $\alpha_1 = 45^\circ$ and $\alpha_2 = 30^\circ$.

where $D_Z(A, E_Z^*, L, t)$ is the probability of population of the DNS configuration $(Z, Z_{\text{CN}} - Z)$ for a given set of E_Z^* and L ; a value of k_{max} corresponds to the interaction time t of the DNS fragments when $D_Z(A, E_Z^*, L, t_{\text{int}}) < 10^{-5}$, *i.e.* the DNS has gone to complete fusion or it has broken up as quasifission products (see Fig. 4). The part of D_Z going to region $Z < 2$ is a contribution to the complete fusion. The evolution of the charge distribution D_Z is calculated by the transport master equation [18] with initial conditions $D_Z(A, E_Z^*, L, t=0) = 1$ for $Z = Z_P(Z_T)$ and $A = A_P(Z_T)$; Λ_Z^{qf} is the width of the decay through the quasifission barrier which is calculated by the expression

$$\Lambda_Z(B^{\text{qf}}(Z, A, \{\alpha_i, \beta_i\}), T_Z(\alpha_i, \beta_i)) \propto \exp\left(\frac{-B_{\text{qf}}(Z, A, \{\alpha_i, \beta_i\})}{T_Z(\alpha_i, \beta_i)}\right), \quad (5)$$

where T_Z is the effective temperature of the DNS with the charge asymmetry Z : $T_Z(A, \alpha_i, \beta_i) = 3.46\sqrt{E_Z^*(A, \alpha_i, \beta_i)/A_{\text{tot}}}$, $A_{\text{tot}} = A_P + A_T$. The transition coefficients of the transport master equation depend on the energy, spin, and occupation numbers of the single-particle states of the nucleons in the DNS fragments (see Refs. [12, 18] for details). The occupation numbers of nucleons in the DNS fragments depend on T_Z .

Evolution of the charge distribution D_Z of the DNS and yield Y_Z of fragments calculated for the $^{16}\text{O}+^{130}\text{Te}$ reaction at $E_{c.m.} = 78.4$ MeV and $L = 40\hbar$ are presented in Fig. 5. The presented results have been obtained for the orientation angles $\alpha_1 = 45^\circ$ and $\alpha_2 = 30^\circ$.

The knowledge of the $Y_Z(Z=2)$ values as a function of $E_{c.m.}$ and L allows us to find the partial cross sections of the incomplete fusion as a very mass asymmetric channel

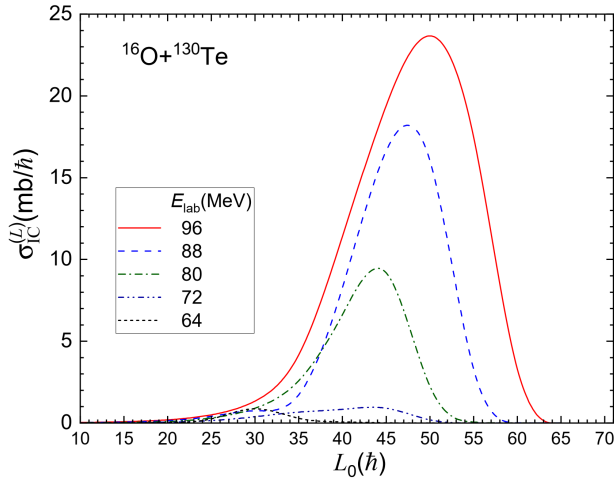


FIG. 6. The partial cross section of the incomplete fusion $\sigma_{ICF}(E_{lab}, L)$ as a function of the angular momentum L for the set of collision energy values E_{lab} for the $^{16}\text{O}+^{130}\text{Te}$ reaction.

of the quasifission process by the following expression:

$$\sigma_{ICF}(E_{c.m.}, L) = \sigma_{cap}(E_{c.m.}, L) * Y_Z(E_{c.m.}, L), \quad (6)$$

where $\sigma_{cap}(E_{lab}, L) = \pi\lambda^2\mathcal{P}_{cap}(E_{lab}, L)$, where λ^2 is the de Broglie wavelength corresponding to the collision energy E_{lab} and \mathcal{P}_{cap} is the capture probability which is found from the calculation of the collision trajectory for the given values of $E_{c.m.}$ and orbital angular momentum L [12].

The increase of the probability of the mass and charge distribution at the $Z = 2$ and $A = 4$ corresponding to the α particle occurs in the collisions with $L = 40\text{--}60 \hbar$ for the $^{16}\text{O}+^{130}\text{Te}$ reaction and in the collisions with $L = 30\text{--}40 \hbar$ for the $^{18}\text{O}+^{93}\text{Nb}$ reaction. These results allow us to make theoretical analysis of the incomplete fusion mechanism by the calculation of the evaporation residues excitation function and to compare with the measured data from Refs. [6, 19].

The partial cross sections of the incomplete fusion for the $^{16}\text{O}+^{130}\text{Te}$ and $^{18}\text{O}+^{93}\text{Nb}$ reactions are presented in Figs. 6 and 7, respectively. The range of the angular momentum values $L = 35\text{--}60 \hbar$ and $L = 25\text{--}40 \hbar$ are favorable for the incomplete mechanism in the first and second reactions, respectively. These ranges are in agreement with the measured averaged values $\langle L \rangle = 40\hbar$ and $\langle L \rangle = 30\hbar$ in the $^{14}\text{N}+^{159}\text{Tb}$ [2] and $^{16}\text{O}+^{146}\text{Nd}$ [3] reactions. The authors of these last two experiments have measured γ -multiplicity to estimate the averaged value of the angular momentum corresponding to the incomplete fusion mechanism.

The other important result are ranges of the DNS excitation energy E_Z^* obtained from the calculations of the capture and fusion cross sections.

The cross sections of the evaporation residues of the nuclei formed at the incomplete fusion are calculated using the DNS excitation energy E_Z^* which decreases due to the increase in the rotational energy of the interacting

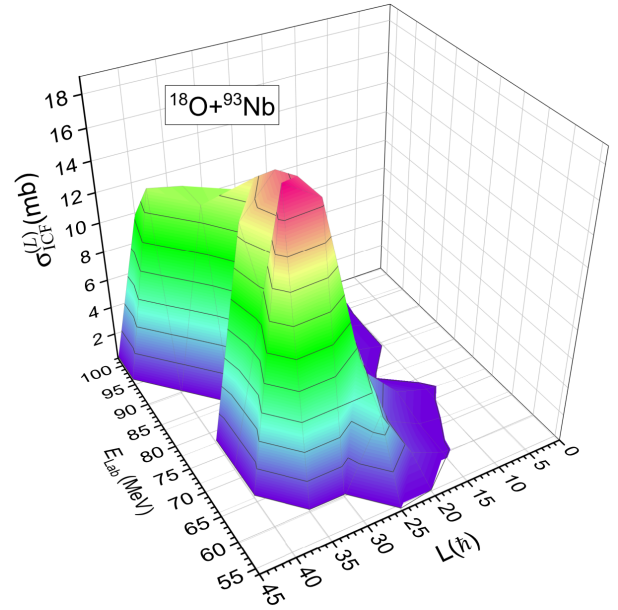


FIG. 7. The partial cross section of the incomplete fusion $\sigma_{ICF}(E_{lab}, L)$ as a function of the angular momentum L for the set of collision energy values E_{lab} for the $^{18}\text{O}+^{93}\text{Nb}$ reaction.

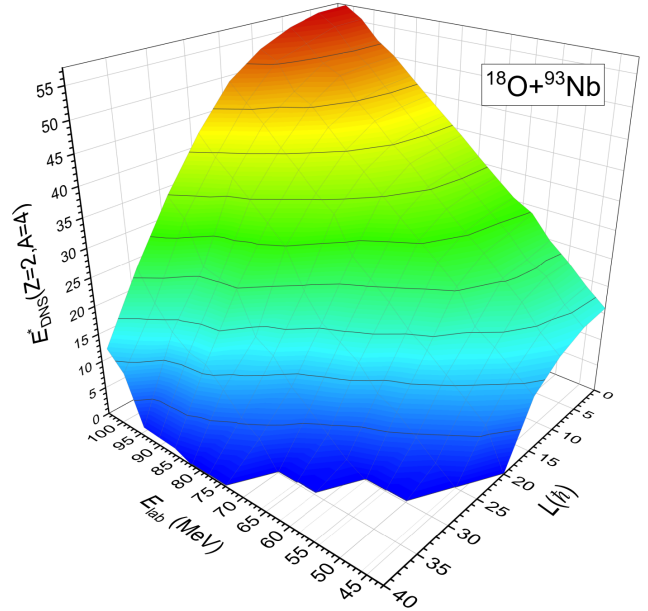


FIG. 8. The range $E_Z^*(E_{lab}, L, \{\beta_i, \alpha_i\}) = 10\text{--}50$ MeV of the DNS excitation energy for the angular momentum $L = 35\text{--}50 \hbar$ leading to the incomplete fusion in the $^{18}\text{O}+^{93}\text{Nb}$ reaction by emission of α particle from the interacting system.

system (see Fig. 8). The important result is the formation of the wide range $E_Z^*(E_{lab}, \ell, \{\beta_i, \alpha_i\}) = 10\text{--}50$ MeV of the DNS excitation energy for the angular momenta $L = 35\text{--}50 \hbar$ of DNS corresponding to the incomplete fusion. The nearly plateau of the excitation function of the evaporation residues of the 1n-5n channels for the wide of the beam energy (65-105 MeV) is related with this

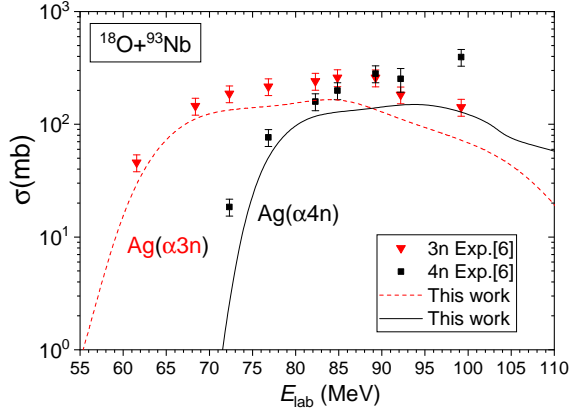


FIG. 9. Comparison of the theoretical cross sections (solid curve) of the evaporation residues formed in the $^{18}\text{O}+^{93}\text{Nb}$ incomplete fusion reaction after emission of 3 neutrons with the measured experimental data (squares) presented in Ref. [6].

phenomenon.

The ER cross sections of the xn channels of the incomplete fusion accompanied with the emission of the α particle have been calculated in the framework of the DNS model [12]. We should note that the excitation energy of the conjugate nucleus after emission of α particle is $E_{\text{ICF}}^*(L) = E_{Z=2}^*(E_{\text{c.m.}}, L, \{\beta_i, \alpha_i\})$ for the given values of orientation angles α_i of the DNS fragments. The evaporation residue (ER) cross section of the xn channel (x neutrons have been emitted) has an excitation energy $E^*(x)$ and its value is calculated a sum of the partial cross sections:

$$\sigma_{\text{ER}}^{(x)}(E^*) = \sum_{\ell=0}^{L_d} (2L+1) \sigma_{\text{ER}}^{(x)*}(\ell, L), \quad (7)$$

where $\sigma_{\text{ER}}^{(x)*}(\ell, L)$ is the partial cross section of the ER formation as the survival cross section of the intermediate nucleus at each step x of the de-excitation cascade by the formula [12, 20]

$$\sigma_{\text{ER}}^{(x)}(E^*, L) = \sigma_{\text{ER}}^{x-1}(E_{x-1}^*, L) W^{(x)}_{\text{sur}}(E_{x-1}^*, L). \quad (8)$$

Here, $\sigma_{\text{ER}}^{x-1}(E_{x-1}^*, L)$ is the partial cross section of the intermediate excited nucleus formation at the $(x-1)$ th step, and $W_{\text{sur}}^{(x)}(E_{x-1}^*, L)$ the survival probability of the x th intermediate nucleus against fission along each step of the de-excitation cascade. It is calculated by the statistical model implanted in KEWPIE2 [21].

Obviously $\sigma_{\text{ER}}^{(0)}(E_{\text{ICF}}^*, L) = \sigma_{\text{ICF}}(E_{\text{ICF}}^*, L)$ which is calculated by (6). This procedure is similar to the calculation of the cross section of the evaporation residues formed after emission of neutrons from the heated and rotating compound nucleus formed at complete fusion [12, 20] where the equation $\sigma_{\text{ER}}^{(0)}(E_{\text{CN}}^*, L) = \sigma_{\text{fus}}(E_{\text{CN}}^*, L)$ was used.

In Fig. 9, the results of calculations using Eq. (7) are compared with the measured cross sections of the

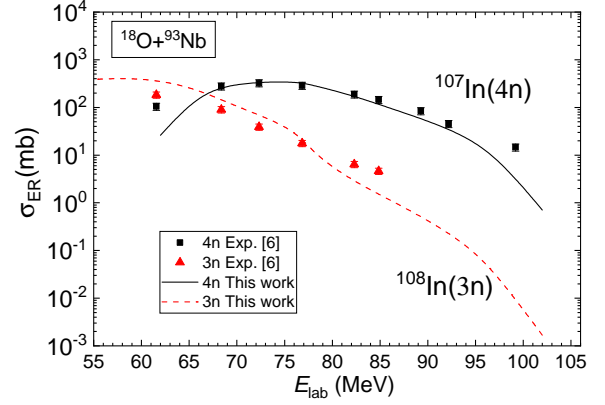


FIG. 10. Comparison of the theoretical cross sections (dashed and solid curves) of the evaporation residues formed in the $^{18}\text{O}+^{93}\text{Nb}$ complete fusion reaction after emission of 3 (triangles) and 4 (squares) neutrons with the measured experimental data presented in Ref. [6].

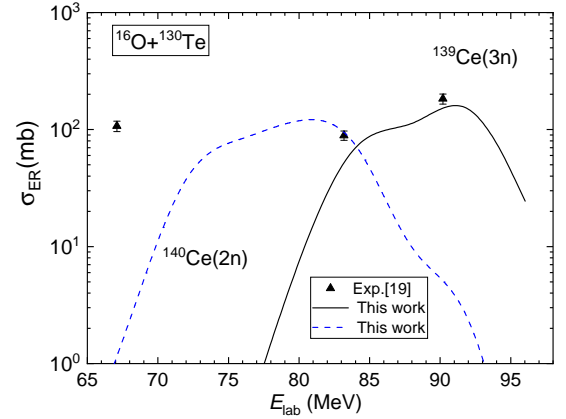


FIG. 11. Comparison of the theoretical cross sections (solid curve) of the evaporation residues formed in the $^{16}\text{O}+^{130}\text{Te}$ complete fusion reaction after emission of 3 neutrons with the measured experimental data (triangles) presented in Ref. [19].

evaporation residues of ^{108}Ag and ^{107}Ag formed in the $^{18}\text{O}+^{93}\text{Nb}$ incomplete fusion reaction after emission of 3 and 4 neutrons [6], respectively. The agreement our results with the measured data is better than that calculated in Ref. [6] by the standard methods ALICE-91 [4] and PACE4 [5, 6].

In Fig. 10, the cross sections of the evaporation residues of ^{107}In and ^{108}In formed in the $^{18}\text{O}+^{93}\text{Nb}$ complete fusion reaction after emission of 4 and 3 neutrons, respectively, are compared with the measured experimental data. It is seen from Fig. 10 that the behaviours of the experimental data and theoretical curves do not have a plateau as a function of the beam energy. From this point of view, the behaviours of the excitation functions of the evaporation residues formed in the incomplete and

complete fusion reactions are different. The difference is explained by increasing the rotational energy $V_{\text{rot}}(Z, L)$ of the DNS with the very mass-asymmetric configuration corresponding to the α -particle emission in collisions with the large beam energies: $V_{\text{rot}}(Z)$ takes an appreciable part of the kinetic energy of the relative motion. As a result, the residual nucleus formed after emission of α -particle in the incomplete fusion is less excited than compound nucleus formed in the complete fusion in heavy-ion collision with the same values of the orbital angular momentum and beam energy. The fission barrier B_f of the heated and rotating compound nucleus decreases due to its large excitation energy E_{CN}^* and angular momentum L .

The theoretical excitation function of the ER ^{139}Ce formed in the incomplete fusion of the $^{16}\text{O}+^{130}\text{Te}$ reaction after emission of the α particle and 3 neutrons is compared with the measured experimental data [19] in Fig. 11. Our approach does not allow us to reach an agreement at low energies where the excitation function of the ER ^{140}Ce formed after emission of the α particle and 2 neutrons dominates over 3n neutron channel.

The new mechanism of the incomplete fusion has been explored as a very mass-asymmetric quasifission of a DNS formed at the capture of the projectile nucleus (full momentum transfer) by the target nucleus. The

L -dependence of the charge distribution of the DNS fragments leads to formation of its configuration consisting of the α particle and a conjugate nucleus. The centrifugal force related with the rotation of a very mass-asymmetric DNS is strong for the $L > 30$. Consequently, it leads to the incomplete fusion which can be considered as the quasifission producing α particle and a conjugate heavy fragment. This phenomenon is related with the transformation of a significant part of the kinetic energy of the collision energy to the rotational energy of the DNS formed at capture of the projectile by target nucleus. As a result the conjugate fragment is less heated than the compound nucleus formed in the complete fusion. Therefore, the plateau of the excitation function of the ER of the 3n-4n channels of the incomplete fusion in the high energy range is observed for the $^{18}\text{O}+^{93}\text{Nb}$ and $^{16}\text{O}+^{130}\text{Te}$ reactions. The measured cross sections of ER formed in the incomplete fusion and complete fusion channels have been reproduced well by the DNS model and the statistical model implanted in KEWPIE2 [21].

Our exploration of the incomplete mechanism has confirmed a decisive role of the orbital angular momentum in the reaction mechanisms of the heavy-ion collisions at energies above the Coulomb barrier and below 10 MeV/nucleon.

-
- [1] W. J. Knox, A. R. Quinton, and C. E. Anderson, *Phys. Rev.* **120**, 2120 (1960).
- [2] T. Inamura, M. Ishihara, T. Fukuda, T. Shimoda, and H. Hiruta, *Physics Letters B* **68**, 51 (1977).
- [3] J. H. Barker, J. R. Beene, M. L. Halbert, D. C. Hensley, M. Jääskeläinen, D. G. Sarantites, and R. Woodward, *Phys. Rev. Lett.* **45**, 424 (1980).
- [4] M. Kumar, A. Agarwal, S. Prajapati, K. Kumar, S. Dutt, I. A. Rizvi, R. Kumar, and A. K. Chaubey, *Phys. Rev. C* **100**, 034616 (2019).
- [5] K. Kumar, T. Ahmad, S. Ali, I. A. Rizvi, A. Agarwal, R. Kumar, K. S. Golda, and A. K. Chaubey, *Phys. Rev. C* **87**, 044608 (2013).
- [6] A. Agarwal, A. K. Jashwal, M. Kumar, S. Prajapati, S. Dutt, M. Gull, I. A. Rizvi, K. Kumar, S. Ali, A. Yadav, R. Kumar, and A. K. Chaubey, *Phys. Rev. C* **103**, 034602 (2021).
- [7] T. Udagawa and T. Tamura, *Phys. Rev. Lett.* **45**, 1311 (1980).
- [8] J. Wilczyński, K. Siwek-Wilczyńska, J. van Driel, S. Gonggrijp, D. C. J. M. Hageman, R. V. F. Janssens, J. Lukasiak, and R. H. Siemssen, *Phys. Rev. Lett.* **45**, 606 (1980).
- [9] J. Wilczyński, K. Siwek-Wilczyńska, J. Van Driel, S. Gonggrijp, D. Hageman, R. Janssens, J. Lukasiak, R. Siemssen, and S. Van Der Werf, *Nuclear Physics A* **373**, 109 (1982).
- [10] R. Van den Bossche and A. Diaz-Torres, *Phys. Rev. C* **100**, 044604 (2019).
- [11] S. N. Kuklin, T. M. Shneidman, G. G. Adamian, and N. V. Antonenko, *Eur. Phys. J. A* **48**, 112 (2012).
- [12] B. M. Kayumov, O. K. Ganiev, A. K. Nasirov, and G. A. Yuldasheva, *Phys. Rev. C* **105**, 014618 (2022).
- [13] G. Audi and A. Wapstra, *Nucl. Phys. A* **595**, 409 (1995).
- [14] P. Möller, J. R. Nix, W. D. Meyers, and W. J. Swiatecki, *At. Data Nucl. Data Tables* **59**, 185 (1995).
- [15] S. Raman, C. Nestor, and P. Tikkanen, *At. Data Nucl. Data Tables* **78**, 1 (2001).
- [16] T. Kibédi and R. Spear, *At. Data Nucl. Data Tables* **80**, 35 (2002).
- [17] A. Nasirov, A. Fukushima, Y. Toyoshima, Y. Aritomo, A. Muminov, S. Kalandarov, and R. Utamuratov, *Nucl. Phys. A* **759**, 342 (2005).
- [18] A. Nasirov, B. Kayumov, and Y. Oh, *Nucl. Phys. A* **946**, 89 (2016).
- [19] D. P. Singh, V. R. Sharma, A. Yadav, P. P. Singh, Unnati, M. K. Sharma, R. Kumar, B. P. Singh, and R. Prasad, *Phys. Rev. C* **89**, 024612 (2014).
- [20] G. Mandaglio, G. Giardina, A. K. Nasirov, and A. Sobczewski, *Phys. Rev. C* **86**, 064607 (2012).
- [21] H. Lü, A. Marchix, Y. Abe, and D. Boilley, *Comput. Phys. Commun.* **200**, 381 (2016).